Wind-Thermal Power System Dispatch Using MLSAD Model and GSOICLW Algorithm

Y.Z. Li[1,2,3], L. Jiang[4], Q.H. Wu[4], P. Wang[5], H.B. Gooi[2], K.C. Li[1],
Y.Q. Liu[3], P. Lu[6], M. Cao[7], J. Imura[8]

[1] State Key Laboratory of Advanced Electromagnetic Engineering and Technology, Huazhong University of Science and Technology, Wuhan 430074, China
[2] School of Electrical and Electronics Engineering, Nanyang Technological University, Singapore 639798, Singapore
[3] State Key Laboratory of Alternate Electrical Power System with Renewable Energy Sources, North China Electric Power University, Beijing 102206, China
[4] Department of Electrical and Electronics Engineering, University of Liverpool, Liverpool L69 3GJ, U.K.
[5] School of Computer Science and Engineering, Nanyang Technological University, Singapore 639798, Singapore
[6] Kunming Engineering Corporation Limited, Kunming, Yunnan 650051, China
[7] Electric Power Research Institute of Yunnan Power Grid, Kunming, Yunnan 650217, China
[8] Graduate School of Information Science and Engineering, Tokyo Institute of Technology, Tokyo 152-8552, Japan

Abstract: The decision support model of mean-lower semi-absolute deviation (MLSAD) and the optimization algorithm of group search optimizer with intraspecific competition and lévy walk (GSOICLW) are presented to solve wind-thermal power system dispatch. MLSAD model takes the profit and downside risk into account simultaneously brought by uncertain wind power. Using a risk tolerance parameter, the model can be converted to a single-optimization problem, which is solved by an improved optimization algorithm, GSOICLW. Afterwards, both the model and the algorithm are tested on a modified IEEE 30-bus power system. Simulation results demonstrate that the MLSAD model can well solve wind-thermal power system dispatch. The study also verifies GSOICLW obtains better convergent dispatching solutions, in comparison with other evolutionary algorithms, such as group search optimizer and particle swarm optimizer.

1. Introduction

Power system dispatch problems (PSDPs) are of great importance for power system operations [40], including optimal power flow (OPF), economic dispatch (ED), etc. PSDPs usually aim to obtain the optimal dispatching solution to realize the minimization of the fuel cost of thermal units [40, 19]. Therefore, PSDP is essentially an optimization problem, and conventional optimization techniques based on mathematical programming have been used for solving it [26, 5, 35].

However, mathematical methods relies on the initial searching solution, and they are easily trapped in local optima. Therefore, evolutionary algorithms (EAs), the heuristic optimization algorithms inspired by natural mechanisms, have been used for solving PSDPs and the results are

promising [2, 8, 17]. In recent years, an algorithm, i.e., group search optimizer (GSO), is proposed by simulating animal searching behavior [9], which is famous for its good global searching ability. However, it shows modest performance on optimizing unimodal functions [9], which demonstrates the local searching ability should be enhanced. Therefore, an improved GSO, GSOICLW, has been proposed to improve its local searching ability [18]. In reference [18], GSOICLW is verified to show better performances than that of GSO by testing against standard benchmark functions.

It is known the utilization of wind energy is a hot issue [10]. However, with more wind power integrated into power grids, optimal dispatching of the wind-thermal power system becomes complex because it is difficult to make prediction of wind power, due to its inherent nature of uncertainty [45, 12]. The fuzzy and the probabilistic methods are the two main methodologies proposed to solve PSDPs with wind power integrated. The former method regards wind power as the fuzzy variable, and can well reflect dispatchers' attitude. However, the final dispatching solution maybe subjected to strong subjectiveness [25, 39].

The probabilistic method is based on the analysis of a specific distribution, e.g., Weibull distribution [10, 31] or Gaussian distribution [15, 1]. However, Weibull distribution describes long-term characteristics of wind speed, therefore, it is not suited to be used for PSDPs [45]. In this way, Gaussian distribution is widely applied to PSDPs [45, 38, 36]. Furthermore, Monte Carlo (M-C) simulation is usually used for generating wind power samples for the stochastic optimization [38, 34, 32]. However, it is noted that the objective function of stochastic optimization problem is usually the mean value of fuel cost, and the corresponding risk brought by uncertain wind power is not considered [7].

The mean-variance (MV) model that measures the profit and risk was proposed in economic investment [24], and this model has been applied in power system dispatching [19, 7, 41]. However, variance is the risk index in MV model, which makes no difference between gains and losses [21]. By and large, behavioural finance studies have consistently found that economic decision-makers try to avoid "pain", i.e., down risk (DR) [13]. DR was first proposed by Roy, who assumed that an investor goal was to minimize his/her potential losses. This kind of potential losses is manifested by the lower semi-deviation [29]. It is noted that even Markowitz, the proposer of the MV model, has stated that mean-lower semi-absolute deviation (MLSAD) model considering both averaged profit and downside risk is more plausible than his MV model [23]. Consequently, we attempt to use downside risk based on MLSAD model to solve PSDPs with wind power.

The contribution of this paper is that we use the MLSAD model for the wind-thermal power system dispatch. In this way, dispatchers can further balance interests of profit and risk in the uncertain environment to determine a suitable dispatching solution. Then this model is converted to a single-optimization problem using the risk tolerance parameter, which becomes a complex optimization problem under uncertainty and an advanced optimization algorithm is needed to solve it. Therefore, the improved algorithm of GSOICLW is applied, and its effectiveness is proved by comparison with other algorithms, such as GSO and particle swarm optimization (PSO). In the end, simulation studies verify the outperformance of MLSAD model and GSOICLW algorithm.

2. Mean-Lower Semi-Absolute Deviation Model for OPF Considering the Integration of Wind Power

2.1. OPF

OPF is one of the most difficult issue for PSDPs, formulated in the following:

$$\begin{aligned} \min \quad & F(x, u) \\ \text{s.t.} \quad & g(x, u) = 0 \\ & h(x, u) \leq 0 \end{aligned} \tag{1}$$

where F is the fuel cost function, x and u stand for state variables and decision variables respectively. g and h are the equality and inequality constrains respectively.

F is formulated as follows:

$$F = \sum_{i=1}^{N_G} c_i P_{G_i}^2 + b_i P_{G_i} + a_i \tag{2}$$

where a_i, b_i and c_i are fuel cost coefficients corresponding to the ith generator, respectively. P_{G_i} is the real power output of the ith generator, and N_G is the number of generators.

x is formulated in the following:

$$x^T = [P_{G_1}, V_{L_1}, \cdots, V_{L_{N_D}}, Q_{G_1}, \cdots, Q_{G_{N_G}}, S_1, \cdots, S_{N_E}] \tag{3}$$

where P_{G_1} is the active power output of the slack bus generator, and V_L represent voltages of load buses. Q_G and S are reactive power outputs of generators and apparent power flows in the grid. N_E is the number of power grid branches.

u are the decision variables:

$$u^T = [P_{G_2} \cdots P_{G_{N_G}}, V_{G_1} \cdots V_{G_{N_G}}, T_1 \cdots T_{N_T}, Q_{C_1} \cdots Q_{C_{N_C}}] \tag{4}$$

where P_G and V_G are active power outputs and voltages of generators respectively. T and Q_C are tap ratios of transformers and power outputs of shunt reactive compensators. N_T and N_C are numbers of transformers and shunt compensators.

$g(x, u)$ requires the power balance in the grid, listed in the following:

$$0 = P_{G_i} - P_{D_i} - V_i \sum_{j=1}^{N_i} V_j (G_{ij} \cos \theta_{ij} + B_{ij} \sin \theta_{ij})$$

$$1 \leq i \leq N_0 \tag{5}$$

$$0 = Q_{G_i} - Q_{D_i} - V_i \sum_{j=1}^{N_i} V_j (G_{ij} \sin \theta_{ij} + B_{ij} \cos \theta_{ij})$$

$$1 \leq i \leq N_{PQ}. \tag{6}$$

3

$h(x, u)$ represents operational limits of a power system:

$$
\begin{aligned}
P_{G_i}^{\min} &\leq P_{G_i} \leq P_{G_i}^{\max} \quad 1 \leq i \leq N_G \\
Q_{G_i}^{\min} &\leq Q_{G_i} \leq Q_{G_i}^{\max} \quad 1 \leq i \leq N_G \\
Q_{C_i}^{\min} &\leq Q_{C_i} \leq Q_{C_i}^{\max} \quad 1 \leq i \leq N_C \\
T_k^{\min} &\leq T_k \leq T_k^{\max} \quad 1 \leq k \leq N_T \\
V_i^{\min} &\leq V_i \leq V_i^{\max} \quad 1 \leq i \leq N_B \\
|S_k| &\leq S_k^{\max} \quad 1 \leq k \leq N_E
\end{aligned} \tag{7}
$$

Nomenclature can be referred to [40].

2.2. MLSAD Model for OPF Considering the Integration of Wind Power

Markowitz firstly proposed the mean-variance (MV) model to deal with the portfolio optimization problem, considering maximization of the profit and minimization of the risk under the uncertain environment [24]. Furthermore, this model has been applied in power system optimization problems [7, 41, 19, 16]. However, variance is the risk index in terms of MV model, which makes no distinction between gains and losses [21]. Behavioural finance studies have consistently found that economic decision-makers try to avoid "pain", i.e., the deviation between of lower profits and expected one [13]. Therefore, the downside risk was proposed in the MLSAD model, which looks at the lower standard deviations of expected returns and tries to avoid potential losses [29]. Due to its advantage, the MLSAD model has been widely used in dealing with portfolio problems [33, 14, 30]. Moreover, even Markowitz, the proposer of the MV model, has admitted that semi-variance is the more plausible measure of risk than his mean-variance theory [23]. As a result, in this paper, the MLSAD model is attempted to solve PSDPs with uncertain wind power integrated.

We set the gap of fuel costs of a power system with and without wind power as the profit function, $R(u)$, and its expectation is expressed as follows:

$$
R(u)^{\exp} = \mathbf{E}_{P_{W_1}, P_{W_2}, \cdots, P_{W_M}} \left\{ \sum_{i=1}^{N_S} (F_0 - F_i) \mathrm{P}(F_i) \right\} \tag{8}
$$

where $\mathbf{E}$ is the expectation operator, M is the number of wind farms, and $(P_{W_1}, P_{W_2}, \cdots, P_{W_M})$ represent active power outputs. N_S is the number of wind power samples corresponding to $P_{W_j}(j = 1, 2, \cdots, M)$ obtained by a sampling method [42]. F_0 is the optimized fuel cost of a power system without wind farms integrated, F_i is the fuel cost as for the ith wind power sample, $(F_0 - F_i)$ then describes the profit brought by wind power. $\mathrm{P}(F_i)$ is the probability of the fuel cost F_i occurs.

On the other hand, the downside risk, i.e., the lower semi-absolute deviation is formulated as:

$$
V_-(u) = \mathbf{E}_{P_{W_1}, P_{W_2}, \cdots, P_{W_M}} \left\{ |R(u) - R(u)^{\exp})|_- \right\} \tag{9}
$$

where $|a|_- = \max\{0, -a\}$.

It can be seen that profits are much lower than the expectation if the value of downside risk is high. Therefore, it is of necessity to take both profit and downside risk into consideration. [7, 41] optimize the mean and variance by using a risk tolerance parameter, converting this model into a single-objective optimization problem. Therefore, in this paper, a risk tolerance parameter, λ, is

also used to analyze the MLSAD model. The objective function is formulated as:

$$\max \quad R^{exp} - \lambda V_- \tag{10}$$

$$\text{s.t.} \quad g(x, u, P_W) = 0 \tag{11}$$

$$h(x, u) \leq 0 \tag{12}$$

where P_W donates active wind power.

Usually, fuel cost is analysed in power systems, therefore, the objective function as below can also be expressed as:

$$\min \quad F^{\text{exp}} + \lambda V_- \tag{13}$$

where

$$F^{\text{exp}} = \mathbf{E}_{P_{W_1}, P_{W_2}, \cdots, P_{W_M}} \sum_{i=1}^{N_S} F_i \mathrm{P}(F_i) \tag{14}$$

F^{exp} means the expectation of fuel cost.

2.3. Wind Power

As OPF is studied in wind-thermal PSDP, the time resolution is one hour [6]. During this resolution, the forecast error $\triangle v$ is proved to follow the Gaussian distribution [15, 45].

$$\triangle v \sim N(0, \sigma_v^2) \tag{15}$$

where $N(0, \sigma_v^2)$ donates Gaussian distribution and the standard deviation is σ_v.

Therefore, the actual wind speed is:

$$v = v_f + \triangle v \tag{16}$$

where v_f is the forecasting value.

The active power of a wind turbine, P_{wt}, is obtained [44]:

$$P_{\text{wt}} = \begin{cases} 0 & 0 \leq v < v_{\text{ci}} \\ \dfrac{P_{\text{ra}} v_{\text{ci}}^3}{v_{\text{ra}}^3 - v_{\text{ci}}^3} + \dfrac{P_{\text{ra}}}{v_{\text{ra}}^3 - v_{\text{ci}}^3} v^3 & v_{\text{ci}} \leq v < v_{\text{ra}} \\ P_{\text{ra}} & v_{\text{ra}} \leq v \leq v_{\text{co}} \\ 0 & v > v_{\text{co}} \end{cases} \tag{17}$$

where v_{ci}, v_{ra}, v_{co} are the cut-in , rated and cut-out wind speed. P_{ra} is the rated power.

When N_{wt} turbines are installed in a wind farm, evidently, the active and reactive power are:

$$P_{\text{farm}} = P_{\text{wt}} \times N_{\text{wt}} \tag{18}$$

$$Q_{\text{farm}} = \frac{P_{\text{farm}}}{\cos\varphi} \sqrt{1 - \cos^2\varphi} \tag{19}$$

where $\cos\varphi$ is the constant power factor.

If the wind farm is integrated into a power system, it will affect the state of power flow. For example, when a wind farm is connected to bus i, power flow equations are changed to:

$$P_{\mathrm{G}i} = P_{\mathrm{D}i} - P_{\mathrm{farm}} + V_i \sum_{j \in N_i} V_j(G_{ij} \cos \theta_{ij} + B_{ij} \sin \theta_{ij}) \tag{20}$$

$$Q_{\mathrm{G}i} = Q_{\mathrm{D}i} - Q_{\mathrm{farm}} + V_i \sum_{j \in N_i} V_j(G_{ij} \sin \theta_{ij} - B_{ij} \cos \theta_{ij}) \tag{21}$$

3. GSOICLW

3.1. GSO

GSO is a recently proposed optimization algorithm, which simulates animals' searching behavior. The producer, scroungers and rangers comprise the searching group. The producer has the best searching ability, and scroungers employ producer-scrounger model [9] to do local searching around the producer. Rangers adopt the searching behavior of random walk to enhance chances to escape local optima. Therefore, GSO outperforms other evolutionary algorithms as for global searching [9].

Each member has their position $\mathbf{X}_i^k \in \mathbb{R}^n$ and a scanning angle $\boldsymbol{\varphi}_i^k = (\varphi_{i1}^k, \varphi_{i2}^k, \cdots, \varphi_{i(n-1)}^k) \in \mathbb{R}^{n-1}$ at the kth iteration, then the unit vector as for the scanning angle $\mathbf{D}_i^k = (d_{i1}^k, d_{i2}^k, \cdots, d_{in}^k) \in \mathbb{R}^n$ is obtained [9]. The formulations of searching regarding these members are shown in the following respectively.

3.1.1. Producer:
The producer, $\mathbf{X}_p^k$, adopts the animal searching behavior by randomly sampling three points, which is formulated as follows.

$$\mathbf{X}_z = \mathbf{X}_p^k + r_1 l_{\max} \mathbf{D}_p^k(\boldsymbol{\varphi}_p^k) \tag{22}$$
$$\mathbf{X}_r = \mathbf{X}_p^k + r_1 l_{\max} \mathbf{D}_p^k(\boldsymbol{\varphi}_p^k + \mathbf{r}_2 \theta_{\max}/2) \tag{23}$$
$$\mathbf{X}_l = \mathbf{X}_p^k + r_1 l_{\max} \mathbf{D}_p^k(\boldsymbol{\varphi}_p^k - \mathbf{r}_2 \theta_{\max}/2) \tag{24}$$

where $\mathbf{X}_z$, $\mathbf{X}_r$ and $\mathbf{X}_l$ are the sampled points. $\boldsymbol{\varphi}_p^k$ is scanning angle, $\theta_{\max} \in \mathbb{R}^1$ and $l_{\max} \in \mathbb{R}^1$ are maximum pursuit angle and distance. $r_1 \in \mathbb{R}^1$ is a standard normally distributed random number and $\mathbf{r}_2 \in \mathbb{R}^{n-1}$ is a uniformly distributed random vector in the range of $(0, 1)$.

When the producer hunts for a better resource, it will fly there. Otherwise, it will take a new randomly scanning angle:

$$\boldsymbol{\varphi}^{k+1} = \boldsymbol{\varphi}^k + \mathbf{r}_2 \alpha_{\max} \tag{25}$$

where $\alpha_{\max} \in \mathbb{R}^1$ is the maximum turning angle.

If the producer cannot hunt for a better resource after a iterations, the scanning angle goes back to zero degree

$$\boldsymbol{\varphi}^{k+a} = \boldsymbol{\varphi}^k \tag{26}$$

where $a \in \mathbb{R}^1$ is a constant.

6

3.1.2. Scroungers and rangers: Scroungers are selected from group members in random, and they perform local searching around the producer, which is formulated as follows.

$$\mathbf{X}_i^{k+1} = \mathbf{X}_i^k + \mathbf{r}_3 \circ (\mathbf{X}_p^k - \mathbf{X}_i^k) \tag{27}$$

where $\mathbf{r}_3 \in \mathbb{R}^n$ is a uniformly distributed random vector in the range of $(0,1)$ and " $\circ$ " is the Hadamard product.

Then rangers adopt random walk, i.e., each ranger moves to a new position by adopting a random head angle φ_i^k and a random distance $ar_1 l_{\max}t$ at the kth iteration.

$$\mathbf{X}_i^{k+1} = \mathbf{X}_i^k + ar_1 l_{\max} \mathbf{D}_i^k(\varphi_i^k) \tag{28}$$

Although GSO shows excellent performance on global searching, while its local searching ability is modest [9]. In order to overcome this drawback, an enhanced GSO, GSOICLW is proposed [18], which incorporates intraspecific competition (IC) [27] and lévy walk (LW) [37] based on GSO.

3.2. Intraspecific Competition

IC comprises contest and scramble competition [27]. In the former one, successful competitor monopolises the resources. The scramble competition happens if competitors are crowded around limited resources, which cannot be monopolized. Therefore, this kind of competition stimulates members to be involved in a serious scramble [3].

In GSO, each member hunts for the optimal resource. As a result, IC exists when members are crowded around the producer. Here we use an index proposed by Zhan [43] to describe crowdedness, f, and detailed calculation are presented:

(1) The mean distance d_i of each particle i with its position x_i to all the other particles is calculated.

$$d_i = \frac{1}{N-1} \sum_{j=1, j \neq i}^{N} \sqrt{\sum_{k=1}^{D}(x_i^k - x_j^k)^2} \tag{29}$$

where N and D are the population size and the number of particles' dimensions.

(2) Then, f can be expressed as

$$f = \frac{d_{\mathrm{g}} - d_{\min}}{d_{\max} - d_{\min}} \in [0,1]. \tag{30}$$

where d_{g} is the d_i as for the leading particle, $d_{\max}$ and $d_{\min}$ are the maximum and minimum distance by comparing all d_i.

It can been seen GSO members are crowded around the producer when f is small. Then IC happens, and $\mathbf{r}_3 = (r_{3_1}, r_{3_2}, \cdots, r_{3_D})$ (called scrounging coefficient), is chosen as higher values to show the serious competition. In GSOICLW, we suppose IC happens if f is less than a constant value, η. Therefore, the value of $\mathbf{r}_3$ is determined by f as follows.

$$r_{3_i} = \begin{cases} \text{random} \in (\zeta, 1) & f < \eta \\ \text{random} \in (0, \zeta) & f \geq \eta \end{cases} \quad i = 1, 2, \cdots, D \tag{31}$$

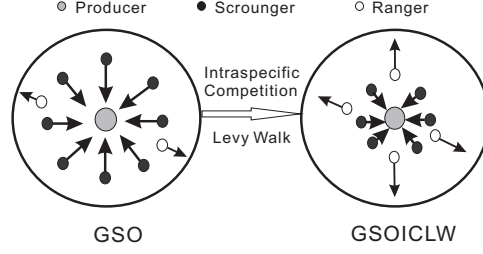where ζ is threshold for the scrounging coefficient to manifest IC.

Fig. 1. *The illustration of GSOICLW*

3.3. Diversifying Effect of IC

IC happens when group members are in crowdedness and competing for a limited resource. Then the diversifying effect will emerge, i.e., the increasing density of IC will make some individuals resort to alternative resources [28]. In this way, more members will hunt for another resource, who become dispersed individuals as rangers [28, 4, 22].

In this way, the diversifying effect will also happen when the group members of GSO are in IC, i.e., some members will become rangers, escaping from the competition. Furthermore, more intense IC, more rangers emerging [28]. As for GSO, the ratio of rangers is a constant of 20%. However, the diversifying effect implies that the proportion of rangers should vary corresponding to the intensity of IC. As a result, the ratio of rangers (donated as c_f) in GSOICLW is expressed as:

$$c(f) = \begin{cases} \dfrac{1}{\alpha + \beta \times \sin(f)} & f < \eta \\ 0.2 & f \geq \eta \end{cases} \tag{32}$$

where α and β are coefficients, they can be determined when programming.

3.4. Lévy Walk

In the algorithm of GSO, rangers adopt RW to hunt for alternative resources. However, it has been proved that LW is of high efficiency, compared with RW [37]. As a result, we set rangers' dispersing behavior to be LW rather than RW, and it is adopted in GSOICLW. Rangers' dispersing length, r, should be drawn from a power-law tail probability distribution function: [37]

$$P(r) \sim r^{-\mu} \quad (1 < \mu < 3). \tag{33}$$

Therefore, the i_{th} ranger moves to:

$$\mathbf{X}_i^{k+1} = \mathbf{X}_i^k + a \cdot r l_{\max} \mathbf{D}_i^k(\boldsymbol{\varphi}^{k+1}) \tag{34}$$

To be concluded, IC and LW are incorporated into GSO shown in Fig. 1. Initially, scroungers follow the producer, and rangers adopt RW to find other resources. When group members are crowded, IC happens and the scrounging coefficient and rangers' ratio varies adaptively. Moreover, it has already been proved GSOICLW outperforms other algorithms, such as GSO [18]. Consequently, we adopt this algorithm to solve the MLSAD model. It is noted that latin hypercube sampling with cholesky decomposition (LHS-CD) is used to sample wind speed forecast errors. The detailed LHS-CD calculation steps can be referred to [42].
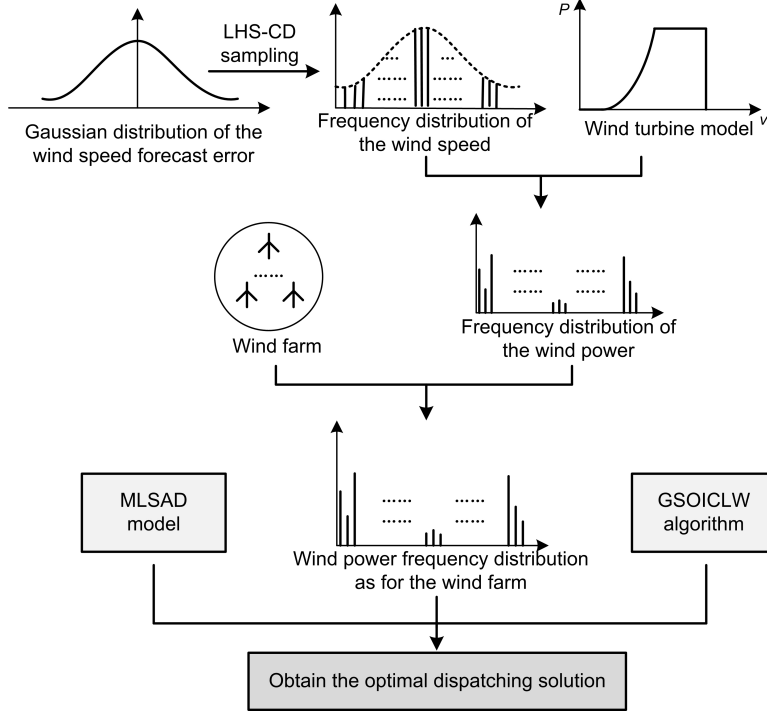
8

Fig. 2. *The framework of obtaining the optimal dispatching solution of wind-thermal power system dispatch*

The procedure of wind-thermal power system dispatch is illustrated in Fig. 2. At the first step, the forecasting error samples of wind speed are obtained by the LHS-CD method, and the frequency distribution is described. Then the frequency distribution and samples of the wind power are also derived. Consequently, the MLSAD model and the algorithm of GSOICLW are applied to to gain the optimal solution, considering both the mean and downside risk.

4. Simulation Studies

To evaluate effectiveness of the MLSAD model and algorithm of GSOICLW, simulation studies are based on a modified IEEE 30-bus power system, which is shown in Fig. 3. For this system, the fuel cost coefficients a_i, b_i and c_i are listed in Table 1. It is assumed that a wind farm with 80 turbines is integrated to the bus 10. Moreover, the predicted wind speed and its standard deviation of forecast error are assumed to be 10 m/s and 8%, respectively. The sampling numbers of LHS-CD is set as 400.
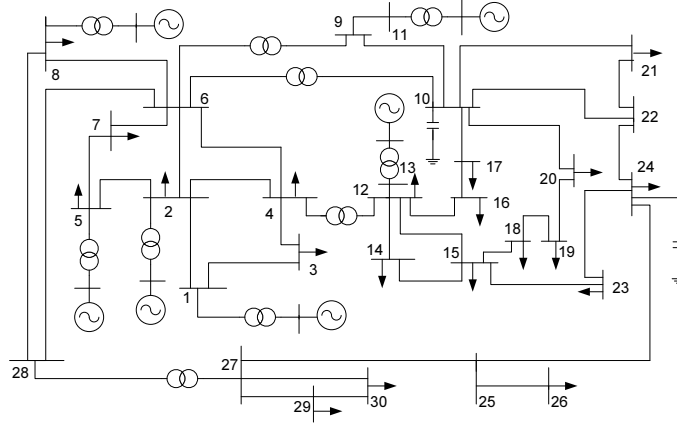
Fig. 3. *IEEE 30-bus power system*

Table 1 Fuel cost coefficients of the test system

Unit	a_i	b_i	c_i	$P^{\max}$	$P^{\min}$
1	0	2	0.00375	250	50
2	0	1.75	0.0175	80	20
3	0	1	0.0625	50	15
4	0	3.25	0.0083	35	10
5	0	3	0.025	30	10
6	0	3	0.025	40	12

Table 2 Results of 3 algorithms in terms of Case I

Algorithms	Best ($/h)	Worst ($/h)	Average ($/h)	Standard deviation	p-value (h-value)
GSOICLW	**532.4**	**533.6**	**533.1**	**0.18**	N/A
GSO	536.6	538.4	537.4	0.39	1.801×10^{-12} (1)
PSO	535.9	540.8	538.1	0.97	2.526×10^{-14} (1)

Two cases are studied, one is to verify the outperformance of GSOICLW on minimization of the fuel cost with predicted wind speed, compared with GSO and PSO. The reason is that it is usual to compare performances of these algorithms to further prove advance of the enhanced one, using experiments [20]. The other aims to test the effectiveness of the MLSAD model, with consideration of uncertainty of wind power.

In the first case, GSOICLW is tested and compared with the other two optimization algorithms, i.e., GSO and PSO, and 50 independent trails and the Mann-Whitney U-test are adopted [11]. The numbers of fitness evaluation for the three algorithms are all set to be 15000. It is known that parameters will affect the performance of optimization algorithms, therefore, we adopt the method of investigating effects of control parameters [9], and obtain the appropriate parameters of IC and LW: $\zeta = 0.8$, $\eta = 0.2$, $\alpha = 2.0$, $\beta = 3.56$ and $\mu = 2$.

4.1. Minimization of fuel cost considering predicted wind speed

This case aims to minimize the fuel cost as shown in (2). It is noted that we use the predicted wind speed on bus 10 rather than uncertain speed. Simulation results, including best, worst, average results and standard deviations of fuel costs obtained by the 3 algorithms as for 50 runs are shown in Table 2 respectively. It is seen GSOICLW obtains better solution as the values of average and standard deviation obtained by this algorithm are 533.1 \$/h and 0.18. In terms of GSO and PSO, the worst results (538.4 \$/h and 540.8 \$/h) and standard deviations (0.39 and 0.97), are much worse than that of GSOICLW. In addition, the gained p-values and h-values of Mann-Whitney U-test show results of GSOICLW are different from the other algorithms. Therefore, it has been proved that GSOICLW outperforms GSO and PSO on OPF with predicted wind speed.

Moreover, Fig. 4 shows the convergent results obtained by these algorithms in the 50 trails. It is verified that results of GSOICLW are more robust. Consequently, the standard deviation in terms of GSOICLW is merely 0.18. Furthermore, to well demonstrate the process of IC, the varying values among 300 iterations of scrounging coefficient (SC) and rangers' ratio are shown in Fig. 5. It is noted that SC is a vector, therefore, the minimum value of this vector is shown in the figure. It can be seen that members of GSOICLW are in IC when the minimum value of SC is bigger than ζ (0.8), and then rangers' ratio are adaptively varying in this phrase.
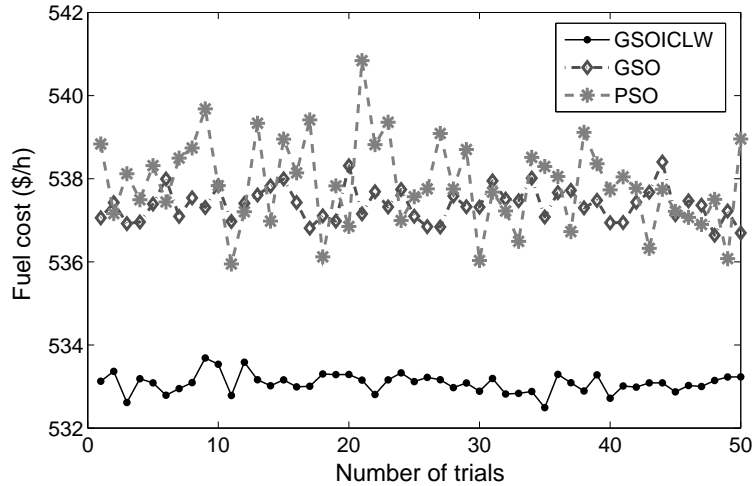

Fig. 4. *The varying paremters in 300 iterations as for GSOICLW*

4.2. Optimization of the MLSAD model with uncertain wind speed

In order to obtain the optimal dispatch solution considering the uncertain wind speed, the MLSAD model is then solved by GSOICLW. By introducing risk tolerance parameter, different weights are assigned to F^{exp} versus the downside risk term V_- shown in (10). λ is set to vary from 0.0 to 0.5. The values of mean and downside risk are obtained and shown in Table 3, and Table 4 lsits the solutions corresponding to difficult risk tolerance parameters. We can see that different levels of risk lead to varying fuel costs. The mean value of fuel cost corresponding to a conservative solution ($\lambda = 0.5$) is 681.5 \$/h while 533.5 \$/h for the aggressive dispatch solution ($\lambda = 0$).

Furthermore, Fig. 6 depicts mean value and semi-absolute deviation (downside risk) versus the risk tolerance parameter, which shows expected fuel cost increases as downside risk decreases. Fig. 7 presents fuel costs corresponding to different wind power samples for solutions A, B and C
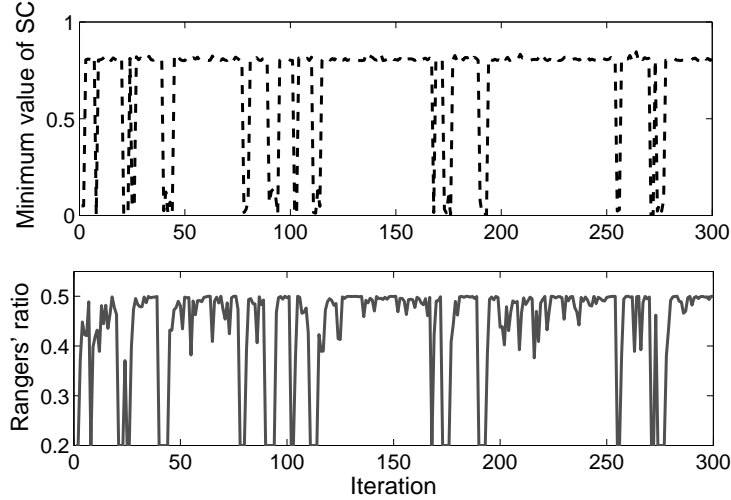
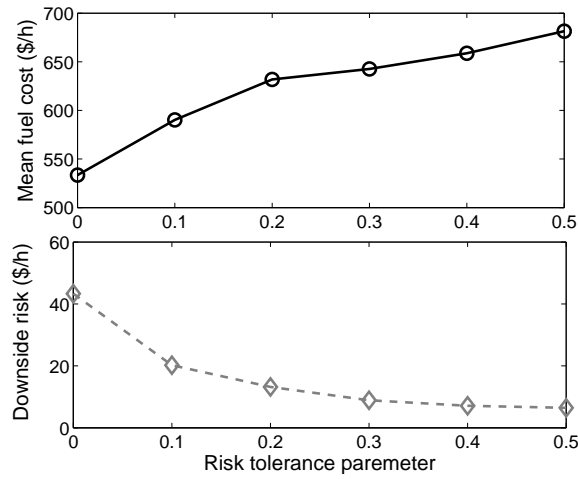**Fig. 5.** *The varying paremters in 300 iterations as for GSOICLW*

Fig. 6. *Values of mean and semi-absolute deviation with different risk tolerance parameters*

when λ is chosen as 0.5, 0.2 and 0.0 respectively. It is noted that in this paper, the downside risk is studied, therefore, the fuel costs which are more than their expectation and imply downside risk, are shown in Fig. 7. It is evident that the averaged fuel cost of C is much less than those of other solutions. However, its semi-absolute deviation is as high as 43.3 $/h, much more that those of other dispatch solutions. This means that solution C cannot well adjust different wind samples, in detail, its high downside risk implies more potential losses. For instance, the values of some fuel costs samples are larger than those of solution B, the 47th, 202th and 264th samples are even more than those of solution A.

Table 3 Values of mean and lower semi-absolute deviation with different risk tolerance parameters

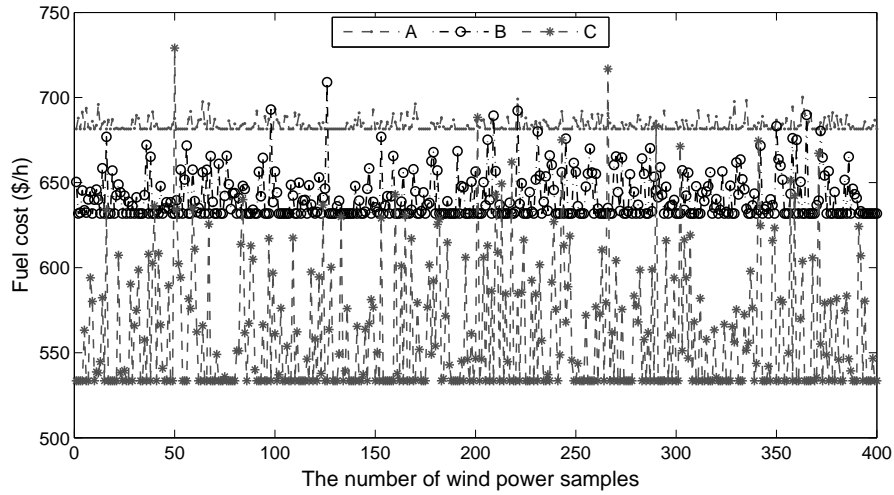| λ	0.0	0.1	0.2	0.3	0.4	0.5
$R(u)^{\mathrm{exp}}$ ($/h)	533.5	590.2	631.8	642.6	658.8	681.5
V_- ($/h)	43.3	20.2	13.2	8.9	7.1	6.4

12

Fig. 7. *Fuel costs samples as for solutions A, B and C*

On the contrary, although the deviation in terms of A is much smaller, its corresponding expected fuel cost is too high, i.e., 681.5 \$/h. For the consideration of economic aspects, it may not be reasonable for dispatchers to select this solution. Based on the discussion above, it is probable that solution B is chosen as a final dispatch solution, to a large extent. To be concluded, power system dispatchers should analyze both the profit and downside risk in terms of wind-thermal power system dispatch problem.

Table 4 The obtained solutions corresponding to difficult risk tolerance parameters

	$\lambda = 0$	$\lambda = 0.1$	$\lambda = 0.2$	$\lambda = 0.3$	$\lambda = 0.4$	$\lambda = 0.5$	Min	Max
P_{G_2}	36.43	45.01	49.59	51.70	52.38	53.15	20	80
P_{G_5}	17.78	20.82	23.53	19.67	19.90	25.64	15	50
P_{G_8}	10.75	15.52	25.24	13.37	12.72	26.76	10	35
$P_{G_{11}}$	10.68	11.17	17.45	12.05	13.19	16.22	10	30
$P_{G_{13}}$	12.32	12.52	15.89	14.36	12.99	23.86	12	40
V_{G_1}	1.0123	1.0221	1.0315	1.0265	1.0443	1.0232	0.95	1.10
V_{G_2}	0.9957	1.0321	1.0372	1.0367	1.0356	1.0321	0.95	1.10
V_{G_5}	0.9850	0.9905	1.0010	0.9973	1.0040	1.0199	0.95	1.10
V_{G_8}	0.9836	0.9922	0.9842	1.0097	1.0001	0.9701	0.95	1.10
$V_{G_{11}}$	1.0392	1.0192	1.0421	1.0912	1.0549	1.0758	0.95	1.10
$V_{G_{13}}$	1.0138	1.0196	1.0268	1.0795	1.0188	1.0693	0.95	1.10
T_{11}	0.9875	0.9625	1.0000	0.9875	0.9875	0.9875	0.90	1.10
T_{12}	0.9625	0.9500	0.9625	0.9625	0.9500	0.9625	0.90	1.10
T_{15}	0.9750	0.9750	1.0000	0.9875	0.9750	0.9875	0.90	1.10
T_{36}	0.9500	0.9875	0.9500	0.9625	0.9500	0.9500	0.90	1.10
$Q_{C_{10}}$	0.04	0.02	0.05	0.04	0.03	0.02	0.00	0.05
$Q_{C_{12}}$	0.05	0.04	0.02	0.05	0.03	0.05	0.00	0.05
$Q_{C_{15}}$	0.04	0.04	0.04	0.05	0.04	0.03	0.00	0.05
$Q_{C_{17}}$	0.02	0.04	0.05	0.05	0.05	0.05	0.00	0.05
$Q_{C_{20}}$	0.04	0.04	0.04	0.04	0.05	0.04	0.00	0.05
$Q_{C_{21}}$	0.04	0.05	0.05	0.05	0.04	0.05	0.00	0.05
$Q_{C_{23}}$	0.02	0.03	0.03	0.02	0.03	0.04	0.00	0.05
$Q_{C_{24}}$	0.04	0.03	0.05	0.05	0.05	0.05	0.00	0.05
$Q_{C_{29}}$	0.03	0.04	0.02	0.03	0.04	0.03	0.00	0.05

5. Conclusion and Further Study

The mean-lower semi-absolute deviation (MLSAD) model has been applied to solve the wind-thermal power system dispatch. It takes the profit and downside risk into account, and GSOICLW is used to solve this complex problem for obtaining the dispatch solution. The simulation study including two cases, the first has tested the performance of GSOICLW on the minimization of the fuel cost considering predicted wind speed, and results have proved that GSOICLW outperforms GSO and PSO. In the other case, the MLSAD model has been optimized by GSOICLW considering uncertain wind speed. Its effectiveness and applicability as for wind-thermal power system dispatch problems have been verified by analysing expected fuel costs and downside risks in terms of different solutions. Further study using the MLSAD model and the GSOICLW algorithm can be investigated in the area of microgrid scheduling, energy network operations, etc.

6. Acknowledgment

7. References

[1] F. Bouffard and F. D. Galiana. Stochastic security for operations planning with significant wind power generation. *IEEE Transactions on Power Systems*, 23(2):306–316, 2008.

[2] A. G. Bakirtzis, P. N. Biskas, C. E. Zoumas, and V. Petridis. Optimal power flow by enhanced genetic algorithm. *IEEE Trans. on Power Syst.*, 17(2):229–236, MAY 2002.

[3] A. A. Berryman. *Principles of Population Dynamics and their Application*. Garland Science, New York, 1999.

[4] D. I. Bolnick. Intraspecific competition favours niche width expansion in drosophila melanogaster. *Nature*, 410:463–466, 2001.

[5] M. H. Bottero, F. D. Galiana, and A. R. Fahmideh-Vojdani. Economic dispatch using the reduced hessian. *IEEE Trans. on Power Appara. Syst.*, 101:3679–3688, Oct. 1982.

[6] M.B. Cain, R.P. O'Neill, and A. Castillio. *History of optimal power flow and formulations*. Federal Energy Regulatory Commission, Washington, DC, 2012.

[7] A. J. Conejo, F. J. Nogales, J. N. Jose, and R. G. Bertrand. Risk-constrained self-scheduling of a thermal power producer. *IEEE Trans. Power Syst.*, 3(3):1569–1574, 2004.

[8] S. He, J. Y. Wen, E. Prempain, Q. H. Wu, J. Fitch, and S. Mann. An improved particle swarm optimization for optimal power flow. *Power System Technology, 2004. PowerCon 2004*, 2:1633–1637, Nov. 2004.

[9] S. He, Q. H. Wu, and J. R. Saunders. Group search optimizer: An optimization algorithm inspired by animal searching behavior. *IEEE Trans. Evol. Comput.*, 13(5):973–990, 2009.

[10] J. Hetzer and D. C. Yu. An economic dispatch model incorporating wind power. *IEEE Trans. on Energy Conversion*, 23(1):603–611, 2008.

[11] M. Hollander and D. A. Wolfe. *Nonparametric Statistical Methods*. John Wiley Sons, New York, 1999.

[12] Y. Y. Hong, H. L. Chang, and C. S. Chiu. Hour ahead wind power and speed forecasting using simultaneous perturbation stochastic approximation (SPSA) algorithm and neural network with fuzzy inputs. *Energy*, 35:3870–3876, 2010.

[13] C. James and P. Michael. Measuring risk for cost of capital: The downside beta approach. *Journal of Corporate Treasury Management*, 4(4):346347, 2012.

[14] H. Konno, H. Waki, and A. Yuuki. Portfolio optimization under lower partial risk measures. *AsiaPac. Financ. Mark.*, 9:127140, 2002.

[15] M. Lange. On the uncertainty of wind power predictions-analysis of the forecast accuracy and statistical distribution of errors. *Journal of Solar Energy Engineering*, 127:177–284, 2005.

[16] M. S. Li, T. Y. Ji, Q. H. Wu, and Y. S. Xue. Stochastic optimal power flow using a paired-bacteria optimizer. *Proc. of IEEE Power Energy Soc. Gen. Meet.*, 2:1–6, July 2011.

[17] Y. Z. Li, M. S. Li, and Q. H. Wu. Energy saving dispatch with complex constraints: Prohibited zones, valve point effect and carbon tax. *Int. J. Electr. Power Energy Syst.*, 72:510–520, 2014.

[18] Y. Z. Li, Q. H. Wu, and M. S. Li. Group search optimizer with intraspecific competition and lévy walk. *Knowledge-Based Systems*, 73:44–51, 2015.

[19] Y. Z. Li, Q. H. Wu, M. S. Li, and J. P. Zhan. Mean-variance model for power system economic dispatch with wind power integrated. *Energy*, 72:510–520, 2014.

[20] J. J. Liang, A. K. Qin, P. N. Suganthan, and S. Baskar. Comprehensive learning particle swarm optimizer for global optimization of multimodal functions. *IEEE Transactions on Evolutionary Computation*, 10(3):2244–2252, 2006.

[21] Y. X. Liu and Z. F. Qin. Mean semi-absolute deviation model for uncertain portfolio optimization problem. *Econometrica*, 6(4):299–307, 2012.

[22] R. C. MacLean. Adaptive radiation in microbial microcosms. *J. Evol. Biol.*, 18:1376–1386, 2005.

[23] H. Markowitz. *Portfolio selection: Efficient diversification of investment*. Blackwell Publishers, Malden, 1991.

[24] H. M. Markowitz. Portfolio selection. *J. Finance*, 8:77–91, 1952.

[25] V. Miranda and P. S. Hang. Economic dispatch model with fuzzy wind constraints and attitudes of dispatchers. *IEEE Trans. Power Syst.*, 20(4):2143–2145, 2005.

[26] R. Mota-Palomino and V.H. Quintana. A penalty function-linear programming method for solving power system constrained economic operation problems. *IEEE Trans. Power Appar. Syst.*, 103(6):1414–1422, 1984.

[27] A. J. Nicholson. An outline of the dynamics of animal populations. *Aust. J. Zoology*, 2:9–65, 1954.

[28] S. Richard and I. B. Daniel. Diversity within a natural population intraspecific competition drives increased resource use diversity within a natural population. *Proc. R. Soc. B.*, 274:839–844, 2007.

[29] A. D. Roy. Safety first and the holding of assets. *Econometrica*, 20(3):431–449, 1952.

[30] J.V. Segura. Fuzzy portfolio optimization under downside risk measures. *Fuzzy Sets and Systems*, 158:769–782, 2007.

[31] L. S. Shi, C. Wang, Y. X. Ni, and M. Bazargan. Optimal power flow solution incorporating wind power. *IEEE Systems J.*, 6(2):233–241, 2012.

[32] H. Siahkali and M. Vakilian. Stochastic unit commitment of wind farms integrated in power system. *Electric Power Systems Research*, 80:1006–1017, 2010.

[33] Y. Simaan. Estimation risk in portfolio selection: the mean vairance model versus the mean absolute deviation model. *Management Science*, 43:1437–1446, 1997.

[34] Y. Z. Sun, J. Wu, and G. J. Li. Dynamic economic dispatch considering wind power penetration based on wind speed forecasting and stochastic programming. *Proceeding of the CSEE*, 29:44–51, 2009.

[35] G. L. Torres and V. H. Quintana. An interior point nonlinear method for nonlinear optimal power flow using voltage retangular coordinates. *IEEE Trans on Power Syst.*, 13:1211–1218, 1998.

[36] B. C. Ummels, M. Gibescu, and E. Pelgrum. Impacts of wind power on thermal generation unit commitment and dispatch. *IEEE Trans. on Energy Conversion*, 22(1):44–51, 2007.

[37] G. M. Viswanathan. Optimizing the success of random searches. *Nature*, 401:911–914, 1999.

[38] J. H. Wang, M. Shahidehpour, and Z. Y. Li. Security-constrained unit commitment with volatile wind power generation. *IEEE Trans. on Power Syst.*, 23(3):1319–1327, 2010.

[39] L. F. Wang and C. Singh. Balancing risk and cost in fuzzy economic dispatch including wind power penetration based on particle swarm optimization. *Electric Power Systems Research*, 78:1361–1368, 2008.

[40] Q. H. Wu and Y. J. Cao. *Dispatching*. Wiley Encyclopedia of Electrical and Electronics Engineering, New York, 1999.

[41] H. Y. Yamin and S. M. Shahidehpour. Risk and profit in self-scheduling for gencos. *IEEE Trans. Power Syst.*, 19(4):2104–2106, 2004.

[42] H. Yu, C. Y. Chung, K. P. Wong, H. W. Lee, and J. H. Zhang. Probabilistic load flow evaluation with hybrid latin hypercube sampling and cholesky decomposition. *IEEE Trans. on Power Syst.*, 24(2):661–667, 2009.

[43] Z. H. Zhan, J. Zhang, Y. Li, and H. S. H. Chung. Adaptive particle swarm optimization. *IEEE Trans. Syst. Man Cybern. B, Cybern.*, 39(6):1362–1381, 2009.

[44] M. Zhao, Z. Chen, and F. Blaabjerg. Probabilistic capacity of a grid connected wind farm based on optimization method. *Renewable Energy*, 31:2171–2187, 2006.

[45] W. Zhou, Y. Peng, and H. Sun. Optimal windthermal coordination dispatch based on risk reserve constraints. *Euro. Trans. Electr. Power*, 21:740–756, 2011.